

Observing ocean heat content using satellite gravity and altimetry

Steven R. Jayne^{1,2} and John M. Wahr

Department of Physics and Cooperative Institute for Research in Environmental Studies, University of Colorado, Boulder, Colorado, USA

Frank O. Bryan

Climate and Global Dynamics Division, National Center for Atmospheric Research, Boulder, Colorado, USA

Received 30 August 2002; revised 30 September 2002; accepted 21 October 2002; published 13 February 2003.

[1] A method for combining satellite altimetry observations with satellite measurements of the Earth's time-varying gravity to give improved estimates of the ocean's heat storage is presented. Over the ocean the time-variable component of the geoid can be related to the time-varying bottom pressure. The methodology of estimating the ocean's time-varying heat storage using altimetric observations alone is modified to include observations of bottom pressure. A detailed error analysis of the methodology is undertaken. It is found that the inclusion of bottom pressure improves the ocean heat storage estimates. The improvement comes from a better estimation of the steric sea surface height by the inclusion of bottom pressure in the calculation, over using the altimeter-observed sea surface height alone. On timescales of the annual cycle and shorter the method works particularly well. However, long-timescale changes in the heat storage are poorly reproduced because of deficiencies in the methodology and the presence of contaminating signals in the bottom pressure observations. *INDEX TERMS*: 4556 Oceanography: Physical: Sea level variations; 1223 Geodesy and Gravity: Ocean/Earth/atmosphere interactions (3339); 1227 Geodesy and Gravity: Planetary geodesy and gravity (5420, 5714, 6019); 1243 Geodesy and Gravity: Space geodetic surveys; 4275 Oceanography: General: Remote sensing and electromagnetic processes (0689); *KEYWORDS*: ocean heat content, altimetry, satellite gravity, steric height, remote sensing

Citation: Jayne, S. R., J. M. Wahr, and F. O. Bryan, Observing ocean heat content using satellite gravity and altimetry, *J. Geophys. Res.*, 108(C2), 3031, doi:10.1029/2002JC001619, 2003.

1. Introduction

[2] The exchange of heat between the ocean and atmosphere is one of the most significant energy transfers within the Earth's climate system. Because of the large heat capacity of water, the ocean can store enormous amounts of energy. Therefore, it can act not only as a moderator of climate extremes, but also as an energy source for severe storms. Indeed, anomalous ocean heat storage in the tropical Pacific Ocean is a hallmark of the El Niño/Southern Oscillation, the largest climate phenomenon outside of the annual cycle. Knowledge of the ocean's time-varying heat storage is of fundamental importance to a host of activities, such as climate change prediction, long-range weather forecasting, hurricane strength prediction, and the Global Climate Observing System. Despite its great importance in climate, however, the ocean's time-varying heat content is vastly

undersampled because of the sparseness of in situ observations, and their concentration in a few geographical areas, mostly along the commercial shipping routes, with a particular bias toward the northern hemisphere. Therefore, accurate satellite mapping of the ocean's time-varying heat storage would be attractive for its global and repeating coverage.

[3] The thermal expansion of seawater associated with the ocean's time-varying heat storage is a large component of the time-varying sea surface height [Gill and Niiler, 1973; Repert *et al.*, 1985]. Previous studies have made use of this fact to estimate the ocean's time-varying heat storage from sea surface heights observed with satellite altimetry [White and Tai, 1995; Hendricks *et al.*, 1996; Wang and Kobinski, 1997; Chambers *et al.*, 1997, 1998; Leuliette and Wahr, 1999; Sato *et al.*, 2000; Polito *et al.*, 2000; Chen *et al.*, 2000; Ferry *et al.*, 2000]. Overall, these studies have found a significant correlation between the estimated heat storage derived from altimetry, and the observed heat storage. Routine observation of the anomalous ocean heat storage for operational monitoring of the Equatorial Pacific Ocean for El Niño relies on using the sea surface height mapped by satellite altimetry.

[4] Observation of the ocean's surface height with satellite altimetry has developed into a mature technique, from

¹Also at Climate and Global Dynamics Division, National Center for Atmospheric Research, Boulder, Colorado, USA.

²Now at Physical Oceanography Department, Woods Hole Oceanographic Institution, Woods Hole, Massachusetts, USA.

its beginnings with GOES-3 and Seasat, through Geosat, to TOPEX/Poseidon, Jason, Geosat Follow-On, ERS-2, Envisat today, and NPOESS in the near future (see *Fu and Chelton* [2001] for a recent review). The current generation of altimetry measurements (i.e., from TOPEX) have a high accuracy, with an RMS error of about 3 cm [*Wunsch and Stammer*, 1998]. On monthly timescales and with spatial and temporal smoothing, the accuracy is even higher, approximately 2 cm [*Cheney et al.*, 1994].

[5] However, despite the high accuracy of the altimeters, there is an essential problem with using the observed sea surface height to estimate the ocean heat content: the altimeter cannot distinguish between steric and nonsteric effects. Therefore, the presence of nonsteric effects degrades the heat storage estimate. Additional observations of the ocean are required, and one of these is an estimate of the ocean bottom pressure which can be provided by satellite gravity observations.

[6] The Gravity Recovery And Climate Experiment (GRACE) mission, sponsored jointly by NASA and the Deutsches Zentrum für Luft-und Raumfahrt, was launched on March 17, 2002, and has a nominal lifetime of five years. The mission consists of two satellites, separated by about 220 km, in identical orbits with initial altitudes near 500 km. The satellites range between each other using a microwave tracking system, and the geocentric position of each spacecraft is monitored using onboard GPS receivers. Onboard accelerometers measure the nongravitational accelerations (i.e., atmospheric drag) so that their effects can be removed from the satellite-to-satellite distance measurements. The residuals will be used to map the Earth's gravity field orders of magnitude more accurately, and to considerably higher spatial resolution, than by any previous satellite. It will provide global maps of the Earth's time-varying gravity field every 30 days and will resolve phenomena at length scales of several hundred km and larger [*Wahr et al.*, 1998; *Hughes et al.*, 2000]. These gravity variations can be used to study a variety of processes that involve redistribution of mass within the Earth or at its surface. Comprehensive descriptions of the expected performance of GRACE and various possible applications are given by *Dickey et al.* [1997] and *Wahr et al.* [1998].

[7] The time-varying component of the gravity field arises largely from the redistribution of water mass around the Earth [*Wahr et al.*, 1998]. On land, changes in water mass are related to changes in soil moisture, aquifer levels and river storage. In the ice sheets, melting of glaciers and ice streamflow redistribute the water mass. In the ocean, local changes in the mass field can arise from two components; changes in sea level and changes in ocean density [*Ponte*, 1999; *Johnson et al.*, 2001].

[8] Through the hydrostatic relation, the change in ocean mass distribution can be directly related to changes in ocean bottom pressure. GRACE is highly accurate over large spatial scales, and it is possible to use these global maps of the time-varying geoid to estimate the ocean bottom pressure on a monthly basis, at a spatial resolution of approximately 500 km, and an accuracy of 1 mm of equivalent sea surface height [*Wahr et al.*, 1998, 2002].

[9] In anticipation of the GRACE gravity data, a method that is used to estimate ocean heat content from satellite altimetry measurements is modified to include satellite

gravity observations. The steric component of sea surface height is related only to the contraction or expansion of seawater, and involves no net change in the vertically integrated mass. Therefore, while steric variability has a sea surface height change associated with it, it does not have an associated gravity signal, a fact that we will utilize here. Other phenomena which reveal themselves in sea surface height variability, such as Rossby waves, Kelvin wave and gravity waves, can also have associated changes in the local ocean mass, and hence will have gravity signals. These distinct signatures in sea surface height and mass change should allow for the separation of the steric sea surface height from the other motions.

[10] In this study we ask whether the estimation of ocean heat storage can be significantly improved by the incorporation of time-variable bottom pressure derived from the GRACE mission, in addition to satellite altimetry. The following section (section 2) discusses the use of satellite gravity and its interpretation as bottom pressure. In section 3, we review the methodology for driving the ocean's heat content from altimetry. We then discuss the application of satellite gravity to observing the ocean and derive a method of estimating heat storage using both altimetry and gravity. In section 4, we illustrate these methods using output from a global ocean general circulation model. In section 5, we perform a detailed estimation of the method's errors. This is followed by a summary and conclusions in section 6.

2. Observing the Ocean Bottom Pressure

2.1. GRACE and the Geoid

[11] It is usual to expand the geoid height, N , as a sum of associated normalized Legendre functions, \tilde{P}_{lm} , in the form [see, e.g., *Chao and Gross*, 1987]:

$$N(\theta, \phi) = a \sum_{l=0}^{\infty} \sum_{m=0}^l \tilde{P}_{lm}(\sin \theta) [C_{lm} \cos(m\phi) + S_{lm} \sin(m\phi)], \quad (1)$$

where the C_{lm} 's and S_{lm} 's are dimensionless Stokes' coefficients, and θ and ϕ are latitude and longitude respectively, and a is the radius of the Earth. GRACE measurements will be used to determine the C_{lm} 's and S_{lm} 's up to degree and order (i.e., l and m) = 100 every 30 days. For each \tilde{P}_{lm} term in this expansion, the horizontal scale (half wavelength) is approximately $20,000/l$ km, (e.g., $l = 40$ corresponds to 500 km).

[12] Observed changes in the C_{lm} 's and S_{lm} 's can be used to learn about variations in the Earth's mass distribution. GRACE will detect changes in the Stokes' coefficients which arise mostly from changes in the distribution of mass within a thin layer at the Earth's surface (for example, in the ocean or atmosphere, or in the storage of water, snow, or ice on continents), with the exception that in certain regions a mass signal from postglacial rebound will contaminate attempts to infer secular mass changes within this thin layer. Define the change in surface mass density, σ' , as the vertical integral of the change in density, ρ' , through this surface layer:

$$\sigma'(\theta, \phi) = \int_{\text{thin layer}} \rho'(\theta, \phi, z) dz \quad (2)$$

where z is the depth through the layer. For an oceanic region, using the hydrostatic relation the change in bottom pressure is $P'_{bot}(\theta, \phi) = g\sigma'(\theta, \phi)$, where g ($=9.8 \text{ m/s}^2$) is the mean gravitational acceleration at the Earth's surface. Using equation (14) of *Wahr et al.* [1998], we find the bottom pressure as a function of the observed Stokes' coefficients:

$$P'_{bot}(\theta, \phi) = \frac{ag\rho_E}{3} \sum_{l=0}^{\infty} \sum_{m=-l}^l \frac{(2l+1)}{(1+k_l)} \tilde{P}_{lm}(\sin\theta) \cdot [C'_{lm} \cos(m\phi) + S'_{lm} \sin(m\phi)], \quad (3)$$

where ρ_E ($= 5517 \text{ kg/m}^3$) is the mean density of the Earth, C'_{lm} and S'_{lm} are the temporal changes in the Stokes' coefficients, and the k_l are load Love numbers representing the response of the solid Earth to surface loads [Farrell, 1972]. Here, we use values of the k_l computed by D. Han (personal communication, 1998), and summarized by *Wahr et al.* [1998, Table 1]. Note that only the temporal change in the bottom pressure can be determined from GRACE. The time mean bottom pressure contributes to the time-averaged geoid which is dominated by the solid Earth contribution and can not be separated from it.

[13] The accuracy of the GRACE C_{lm} and S_{lm} solutions decreases quickly enough at large l , that the use of (3) as written leads to inaccurate results. Instead, the GRACE data will best be used to provide spatial averages of P'_{bot} . Methods of constructing optimal averages for regions of arbitrary size and shape are described by *Swenson and Wahr* [2002] and S. Swenson et al. (Estimated accuracies of regional water storage anomalies inferred from GRACE, submitted to *Water Resources Research*, 2002). Here, instead, we use a simpler averaging method, described by *Wahr et al.* [1998].

[14] Define a Gaussian spatial-averaging kernel as

$$W(\gamma) = \frac{b \exp[-b(1 - \cos \gamma)]}{2\pi (1 - e^{-2b})} \quad (4)$$

[Jekeli, 1980], where γ can be any angle between 0 and 2π , and

$$b = \frac{\ln(2)}{\left(1 - \cos\left(\frac{r_{\frac{1}{2}}}{a}\right)\right)}. \quad (5)$$

Here, $r_{\frac{1}{2}}$ is the half width of the Gaussian averaging function: i.e., when $\gamma = r_{\frac{1}{2}}/a$, $W(\gamma)$ has decreased to half its value at $\gamma = 0$.

[15] We define

$$\overline{P'_{bot}}(\theta, \phi) = \int W(\gamma) P'_{bot}(\theta', \phi') \cos \theta' \sin \theta' dA' \quad (6)$$

where now γ is the angle between the points (θ, ϕ) and (θ', ϕ') (i.e., $\cos \gamma = \sin \theta \sin \theta' + \cos \theta \cos \theta' \cos(\phi - \phi')$), and dA' is an element of solid angle ($dA' = \sin \theta' d\theta' d\phi'$). We refer to $\overline{P'_{bot}}$ as the spatial average of P'_{bot} . Using the expansion (3) in (6), we obtain

$$\overline{P'_{bot}}(\theta, \phi) = \frac{ag\rho_E}{3} \sum_{l=0}^L \sum_{m=-l}^l W_l P_{lm}(\sin\theta) \cdot [C_{lm} \cos(m\phi) + S_{lm} \sin(m\phi)] \quad (7)$$

Table 1. Expected RMS Error of the GRACE Retrieval as a Function of the Averaging Radius^a

Averaging Radius $r_{\frac{1}{2}}$, km	RMS Error of Bottom Pressure Retrieval, mbar
200	10.06
300	0.58
400	0.16
500	0.09
600	0.06
700	0.04
800	0.03

^aHere 1 mbar = 100 Newton/m² \approx 1 cm of sea surface height.

where

$$W_l = \int_0^\pi W(\alpha) P_l(\cos \alpha) \sin \alpha d\alpha \quad (8)$$

and $P_l = \tilde{P}_{lm} = P_l(\cos \alpha)$ are the Legendre polynomials. The summation in (7) is cutoff at degree L , the upper limit of the Stokes' coefficients provided by GRACE which is expected to be around $L \approx 100$. Recursion relations useful for finding the W_l 's are derived by *Jekeli* [1980] and summarized in equation (34) of *Wahr et al.* [1998]. A large value of $r_{\frac{1}{2}}$ in (5) causes the W_l 's to decrease rapidly with increasing l , so that contamination from inaccurate GRACE results for C_{lm} and S_{lm} at large l is suppressed in (7).

[16] Values of the averaging radius, $r_{\frac{1}{2}}$, in the range of 300–700 km and larger give acceptable errors in the mass retrievals, depending on the application. Using estimated errors for the GRACE retrievals consistent with those described by *Jet Propulsion Laboratory* [2001] and provided by B. Thomas and M. Watkins (JPL, personal communication, 1998), we estimate RMS errors in the estimation of the spatially averaged time-varying bottom pressure from the satellite measurement errors in the range of 0.04–0.58 mbar (1 mbar = 100 Newton/m² \approx 1 cm of sea surface height) as summarized in Table 1. The errors at 300 km averaging radius (RMS error of 0.58 mbar) are 6 times larger than the errors at 500 km (RMS error of 0.09 mbar), therefore we have selected 500 km as the averaging radius throughout this analysis. Other sources of error in the estimation of ocean bottom pressure will come from leakage of the hydrological signal over land that will contaminate the ocean signal near the coasts, and postglacial rebound which will degrade the secular estimates at high latitudes.

2.2. Bottom Pressure Variability

[17] Both barotropic and baroclinic motions have bottom pressure signatures, and therefore will be measured by GRACE. We ask how their respective bottom pressure and sea surface heights scale; that is, will the barotropic mode or baroclinic mode dominate the bottom pressure variability?

[18] We begin by considering a two layer fluid as by *Gill* [1982], which has an upper layer density of $\rho_0 - \Delta\rho$, and a lower layer of density ρ_0 (with $\Delta\rho/\rho_0 \ll 1$), with equilibrium depths h_1 and h_2 respectively. Suppose that at time t and location (x, y) , the ocean's surface and the boundary between the upper and lower layers are displaced upward by the amounts $\eta(x, y, t)$ and $\xi(x, y, t)$, respectively (see Figure 1). Let $\eta'(x, y, t)$ and $\xi'(x, y, t)$ be the departures of η and ξ from

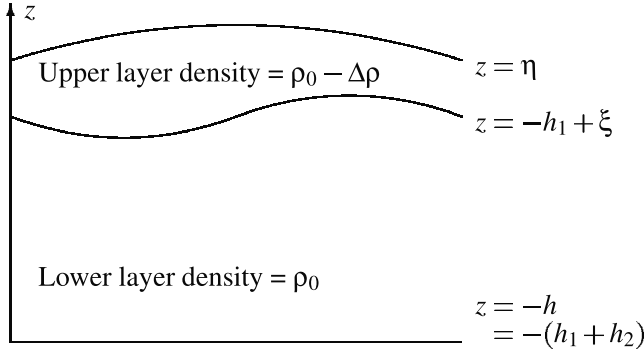


Figure 1. Schematic of a simple two layer fluid.

their time-averaged means. Then using hydrostatic balance, the deviation from the time mean bottom pressure is

$$P'_{bot} = \eta' g(\rho_0 - \Delta\rho) + \xi' g \Delta\rho. \quad (9)$$

For barotropic motions, $\xi' \approx \eta' h_2/h$, where $h = h_1 + h_2$ is the depth of the ocean [Gill, 1982]. So for a barotropic sea surface height deviation, η' , the corresponding bottom pressure perturbation is given by:

$$\begin{aligned} P'_{bot} &= \eta' g(\rho_0 - \Delta\rho) + \eta' g \frac{h_2}{h} \Delta\rho \\ &= \eta' g \rho_0 \left(1 - \frac{\Delta\rho}{\rho_0} + \frac{h_2}{h} \frac{\Delta\rho}{\rho_0}\right) \\ &= \eta' g \rho_0 \left(1 - \frac{\Delta\rho}{\rho_0} \frac{h_1}{h}\right) \\ &\approx \eta' g \rho_0. \end{aligned} \quad (10)$$

For baroclinic motions, $\xi' \approx -\eta' \rho_0 h / (\Delta\rho h_2)$ [Gill, 1982]. So, for a baroclinic deviation in sea surface height, the bottom pressure change is given by:

$$\begin{aligned} P'_{bot} &= \eta' g(\rho_0 - \Delta\rho) - \eta' g \rho_0 \frac{h}{h_2} \\ &= \eta' g \rho_0 \left(1 - \frac{\Delta\rho}{\rho_0} - \frac{h}{h_2}\right) \\ &\approx \eta' g \rho_0 \left(\frac{h_2}{h_2} - \frac{h_1 + h_2}{h_2}\right) \\ &\approx -\eta' g \rho_0 \frac{h_1}{h_2}. \end{aligned} \quad (11)$$

For an upper layer that is sufficiently thinner than the lower layer (i.e., $h_1 \ll h_2$, which is the case for most of the ocean), the baroclinic contribution to bottom pressure will be proportionally smaller, by a factor of h_1/h_2 , than the barotropic contribution to bottom pressure for an equivalent change in sea surface height. Therefore, compared to an altimeter, GRACE will be more sensitive to barotropic fluctuations than to baroclinic ones.

3. Methodology

3.1. Steric Sea Surface Height

[19] Chambers *et al.* [1997] demonstrated a method for calculating the ocean's heat storage from observations of the

sea surface height. Starting from thermodynamic relationships, they made a series of approximations to enable them to calculate ocean heat storage from sea surface height, as measured by satellite altimetry. The steric height, η_{st} , is the vertical integral over some layer thickness, h , of the specific volume anomaly and can be related to the ocean's density field in approximate form as [Tomczak and Godfrey, 1994]:

$$\begin{aligned} \eta_{st}(\theta, \phi, t) &= \int_{-h}^{\eta} \left(\frac{1}{\rho(\theta, \phi, z, t)} - \frac{1}{\rho_0} \right) \rho_0 dz \\ &\approx -\frac{1}{\rho_0} \int_{-h}^{\eta} [\rho(\theta, \phi, z, t) - \rho_0] dz, \end{aligned} \quad (12)$$

in the limit of $|\rho(z) - \rho_0|/\rho_0 \ll 1$, where ρ_0 is the reference density and $\rho(z)$ is the density as a function of depth. The time variable part of the steric height can be written as:

$$\begin{aligned} \eta'_{st} &= \eta_{st} - \bar{\eta}_{st} = -\frac{1}{\rho_0} \int_{-h}^{\eta} [\rho(\theta, \phi, z, t) - \rho_0] dz \\ &\quad + \frac{1}{\rho_0} \int_{-h}^{\eta} [\bar{\rho}(\theta, \phi, z) - \rho_0] dz, \end{aligned} \quad (13)$$

then

$$\eta'_{st} = -\frac{1}{\rho_0} \int_{-h}^{\eta} [\rho(\theta, \phi, z, t) - \bar{\rho}(\theta, \phi, z)] dz \quad (14)$$

where $\bar{\rho}$ is the time mean density as a function of longitude, latitude, and depth. Decomposing the density deviations into a part owing to temperature variations, T' , and a part owing to salinity variations, S' , gives,

$$\eta'_{st}(\theta, \phi, t) = -\frac{1}{\rho_0} \left[\int_{-h}^{\eta} \frac{\partial \rho}{\partial T} T'(\theta, \phi, z, t) dz + \int_{-h}^{\eta} \frac{\partial \rho}{\partial S} S'(\theta, \phi, z, t) dz \right]. \quad (15)$$

The change in steric height on seasonal timescales is to first order a reflection of the thermal changes in the water column. Haline effects may play a nonnegligible role in a few locations, like the western tropical Pacific [Maes, 1998]. However, removing the haline contribution requires concurrent salinity observations since corrections based on climatologies [i.e., Levitus *et al.*, 1994] can actually degrade the accuracy of the correction [Sato *et al.*, 2000]. Therefore, consistent with Chambers *et al.* [1997] and Chen *et al.* [2000], we drop the haline contribution to the steric sea surface height. Neglecting the effect of haline expansion on the steric sea level leaves,

$$\eta'_{st}(\theta, \phi, t) = \int_{-h}^{\eta} \alpha(\theta, \phi, z, t) T'(\theta, \phi, z, t) dz \quad (16)$$

where,

$$\alpha = -\frac{1}{\rho_0} \frac{\partial \rho}{\partial T}, \quad (17)$$

is the thermal expansion coefficient of seawater. A final approximation is required here, and that is that the thermal expansion coefficient, α , is constant over the depth of

heating, and can be taken out of the integral. These assumptions introduce errors, but they are not large, as will be demonstrated in section 5. To first order then, we obtain a relation for the steric height anomaly in terms of a temperature change over some depth integral:

$$\eta'_{st}(\theta, \phi, t) = \alpha_0(\theta, \phi, t) \int_{-h}^{\eta} T'(\theta, \phi, z, t) dz, \quad (18)$$

where α_0 is the depth-independent approximation used for α .

3.2. Thermal Expansion

[20] In a similar manner, the change in ocean heat storage (H') is related to the temperature change over the same layer by:

$$H'(\theta, \phi, t) = \int_{-h}^{\eta} \rho(\theta, \phi, z, t) c_p(\theta, \phi, z, t) T'(\theta, \phi, z, t) dz, \quad (19)$$

where c_p is the heat capacity of seawater. The product of density and heat capacity is very nearly constant (varying by less than 1% over a wide range of temperatures and salinities), and can be taken out of the depth integral leaving,

$$H'(\theta, \phi, t) = \rho c_p \int_{-h}^{\eta} T'(\theta, \phi, z, t) dz. \quad (20)$$

Relating the heat storage anomaly (20) to the steric height anomaly (18) gives us a relation for the change in heat storage relative to the time-varying sea surface height,

$$H' = \frac{\rho c_p}{\alpha_0} \eta'_{st}. \quad (21)$$

Notice that the unknown depth, h , drops out of the integral, and indeed no assumptions need be made about where in the water column that the change in the temperature takes place, as even temperature changes in the deep ocean can change the steric sea surface height.

[21] The numerical values of the thermal expansion coefficient, α , can be inferred by purely statistical methods [White and Tai, 1995], in which in situ observations of the temperature profile are correlated to observed sea surface height changes, and then expanded in time and space to cover unsampled regions. Alternatively, Chambers *et al.* [1997] estimated α using the thermodynamic quantities calculated from temperature and salinity distributions from the climatology of Levitus *et al.* [1994] and Levitus and Boyer [1994]. They then calculated heat storage anomalies from the sea surface height anomalies observed by TOPEX/Poseidon, using the altimeter-observed sea surface heights (corrected for the inverted barometer effect and the tides) in place of the steric height in (21). Overall, they achieved good agreement between their annual cycle of heat storage and that calculated from the Levitus and Boyer [1994] database. Chambers *et al.* [1997] found that in low latitudes to midlatitudes the accuracy of the heat storage rate for the annual cycle was found to be better than 30 W/m^2 (or equivalently $150 \times 10^6 \text{ J/m}^2$ in heat storage), compared to the amplitude of the annual cycle of $50\text{--}100 \text{ W/m}^2$.

Furthermore, they showed that interannual heat storage rates estimated from the altimetry agreed with direct observations from the TOGA-TAO array in the Equatorial Pacific Ocean. Overall, this method based on approximations to first principles showed a similar accuracy at retrieving heat storage from altimetry as those based on purely statistical inferences [i.e., White and Tai, 1995].

[22] A complementary methodology was employed by Stammer [1997] to estimate the steric sea level so that it could be removed from TOPEX/Poseidon altimetric observations. In that work, estimates of the steric sea level were computed from the relation:

$$\frac{\partial \eta_{st}}{\partial t} = \frac{\alpha Q}{\rho c_p}, \quad (22)$$

where Q is the surface heat flux from meteorological analyses. This estimate of the steric surface height was compared to the annual cycle of the sea surface height observed from TOPEX/Poseidon. He concluded that the observed height changes are indeed dominated by thermal expansion arising from the surface heat flux on annual and longer time scales. Wang and Koblinski [1997] also used an equation similar to (22) to estimate the large-scale, air-sea heat flux from the time rate of change of sea surface height as measured by the altimeter, as an alternative to using the bulk formula to estimate the air-sea heat flux.

[23] However, a fundamental problem with these methods remains their inability to take into account the difference between the observed sea surface height and the steric sea surface height. That is they assume that other signals in the sea surface height (i.e., barotropic variability) are negligible and lead to small errors in the heat storage estimation [Chambers *et al.*, 1997]. Vivier *et al.* [1999] found that in addition to steric sea surface height changes, Ekman pumping, equatorially trapped Kelvin waves, and baroclinic Rossby waves were all significant contributors to the changing sea surface height. In the midlatitude to high-latitude barotropic effects have been found to be large [Fukumori *et al.*, 1998], and indeed Chambers *et al.* [1997] found one of their major sources of error was the unknown contribution to the observed sea surface height variability by barotropic fluctuations. They estimated that the barotropic variability introduced an error of order 30 W/m^2 (or equivalently $150 \times 10^6 \text{ J/m}^2$ in heat storage), equivalent to an error about 50% larger than errors in heat storage estimated directly from hydrography. Since it is not a good assumption to neglect nonsteric height variability in some regions of the ocean, we pose the question: Does the addition of bottom pressure observations improve the estimation of ocean heat storage determined from altimetry?

3.3. Combining Sea Surface and Bottom Pressure

[24] The ocean's time-varying component of the mass field is related to the time-varying bottom pressure, by the hydrostatic relation:

$$P_{bot}(\theta, \phi, t) = \int_{-H}^{\eta(t)} g\rho(\theta, \phi, z, t) dz \quad (23)$$

The time-varying component of bottom pressure, is:

$$P'_{bot}(t) = \int_{-H}^{\eta(t)} g\rho'(z, t) dz + \eta'(t)g\rho_0. \quad (24)$$

Rearranging (24), and using (12), gives:

$$\eta'(t) - \frac{1}{g\rho_0}P'_{bot}(t) = -\frac{1}{\rho_0} \int_{-H}^{\eta(t)} \rho'(z,t) dz \approx \eta'_{st}. \quad (25)$$

Therefore, the steric sea surface height is merely the observed sea surface height minus the scaled bottom pressure.

[25] Following the same derivation as presented above, (21) is then modified to include the time-varying bottom pressure, so that the heat content can be related to the sea surface height (corrected for the tides and inverted barometer effect) and bottom pressure by:

$$H' = \frac{\rho C_p}{\alpha} \left(\eta' - \frac{1}{g\rho_0}P'_{bot} \right). \quad (26)$$

Now instead of using only the observed sea surface height and assuming that it adequately represents the steric sea surface height, a more precise representation can be found by combining the observed sea surface height with the bottom pressure observed by GRACE. In the following section we explore whether the modified method (26) provides improved heat storage estimates over using (21).

4. Results

[26] As the GRACE satellite was only recently launched in spring 2002 and has not yet returned science data, we utilize output from a numerical model as a proxy for ocean observations to test the methodology for estimating the ocean heat storage from satellite altimetry and gravity data. This analysis also provides an estimation of the inherent errors in the methodology and provides a measure of how well the heat content estimation procedure will work with real data. For this work we use output from a free surface, primitive equation, global ocean general circulation model (the POP model of *Dukowicz and Smith* [1994]) configured on a grid with average horizontal resolution of ≈ 65 km, and with 40 vertical levels separated by 10 m near the surface to 250 m in the deep ocean. Horizontal dissipation is provided by an anisotropic Smagorinsky eddy viscosity [*Smagorinsky*, 1963; *Smith and McWilliams*, 2002] with coefficients that vary in the along-flow and cross-flow directions. Bottom friction is parameterized with a quadratic bottom drag with a coefficient of 10^{-3} . Vertical viscosity is calculated from the K profile parameterization following *Large et al.* [1994], and the effects of sub-grid-scale eddies are parameterized as by *Gent and McWilliams* [1990]. The model is driven by 6-hourly values of wind stress, surface heat flux, and surface virtual salt flux generated from the reanalysis product from the National Centers for Environmental Prediction (NCEP) as described by *Large et al.* [1997] (though it should be noted that some of the environmental parameters used to compute the fluxes are based on longer-term averages, namely the cloud fraction and precipitation are from monthly averaged observations, and ice fraction is from daily averaged observations). The model was initialized from climatology and integrated forward in time from January 1, 1958, for 43 simulated years. In this study we use the model results for the period January 1993

through December 1997 to simulate a nominal 5-year mission. The analyses presented in this section provide a gauge of the accuracy with which the heat storage variability, could be estimated given perfect sea surface height and bottom pressure observations. The errors in the estimates here come solely from the mathematical approximations and physical assumptions made in section 3; observational errors will be discussed in section 5.

[27] The ocean model was sampled to obtain the sea surface height, bottom pressure, sea surface temperature and salinity, and vertically integrated temperature field. All the data were averaged to 1 month intervals, which is the nominal GRACE sampling interval. The thermal expansion coefficient was calculated from the monthly averaged sea surface salinity and temperature, as by *Chambers et al.* [1997]. Since the ocean model (POP) that was used for this analysis is a Boussinesq model, that is it is volume-conserving rather than mass-conserving, the bottom pressure was corrected using the method described by *Greatbatch* [1994]. Finally, all the variables were spatially averaged with a Gaussian weighting function with a half width of 500 km (see section 2.1, above) onto a 1° grid. Figure 1 shows the root mean square (RMS) variability of the monthly averages of the sea surface height and bottom pressure (scaled by density and gravity into equivalent sea surface height). The sea surface height variance on monthly and longer timescales is dominated by the western boundary currents and the tropics. The bottom pressure on the other hand has energetic areas in the North Pacific Ocean, the Southern Ocean southeast of Australia (in the Bellingshausen and Mornington Basins) and southwest of Australia (in the Australian-Antarctic Basin) where there are large wind- and pressure-driven barotropic fluctuations. These regions are the same as those discussed by *Tierney et al.* [2000] and *Stammer et al.* [2000] for the potential aliasing problems that they present for altimeters and GRACE observations. The high-frequency (less than 60-day period) barotropic variability at these sites is large and is aliased by the satellite's monthly sampling characteristics.

[28] The time series of model sea surface heights were used to calculate monthly maps of the expected change in ocean heat content using (21) together with the thermal expansion coefficient calculated from the monthly mean values of sea surface temperature and salinity. The heat content estimation was then repeated using (26) with both the bottom pressure and sea surface height. These estimates of the heat storage were then compared to the time series of the "true" heat storage calculated directly from the depth integral of the temperature field. The RMS of the monthly heat storage values as a function of latitude and longitude are shown in Figure 2a.

[29] Several features are noteworthy: the large variations in heat storage in the Equatorial Pacific stand out in particular, as does the significant heat storage variability in the North Atlantic (over the Gulf Stream) and the North Pacific (over the Kuroshio extension). Figure 2b shows the RMS difference between monthly values of the true model heat storage and those estimated using only the model's sea surface height and (21). It is immediately seen that the estimated heat storage using the sea surface height alone readily captures the variability in the tropical areas. This is because barotropic variability is small there [*Chao and Fu*,

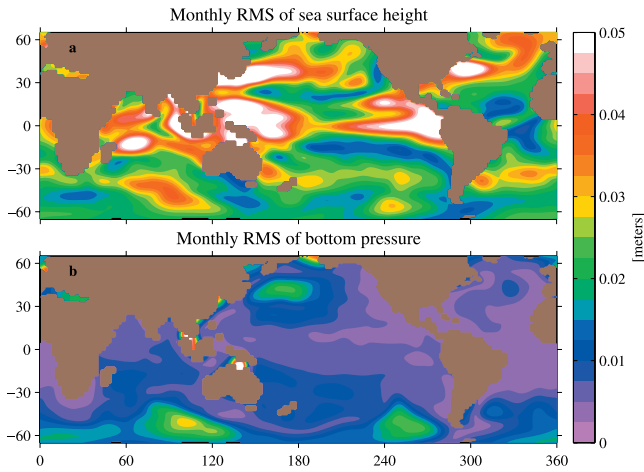


Figure 2. (a) RMS of monthly change in sea surface height from the model. (b) RMS of monthly change in the bottom pressure from the model. The bottom pressure has been divided by the reference density times gravity so that both are in units of meters.

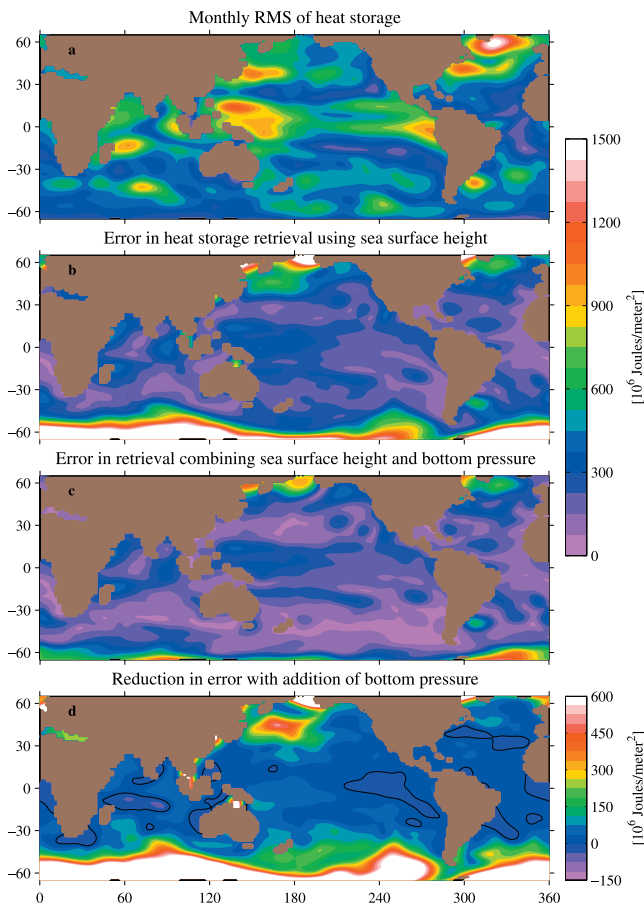


Figure 3. (a) RMS of monthly change in heat storage from the model. (b) Error in heat storage calculated using sea surface height alone. (c) Error in heat storage when using sea surface height combined with bottom pressure. (d) RMS difference in the errors when using sea surface height alone and when combined with bottom pressure.

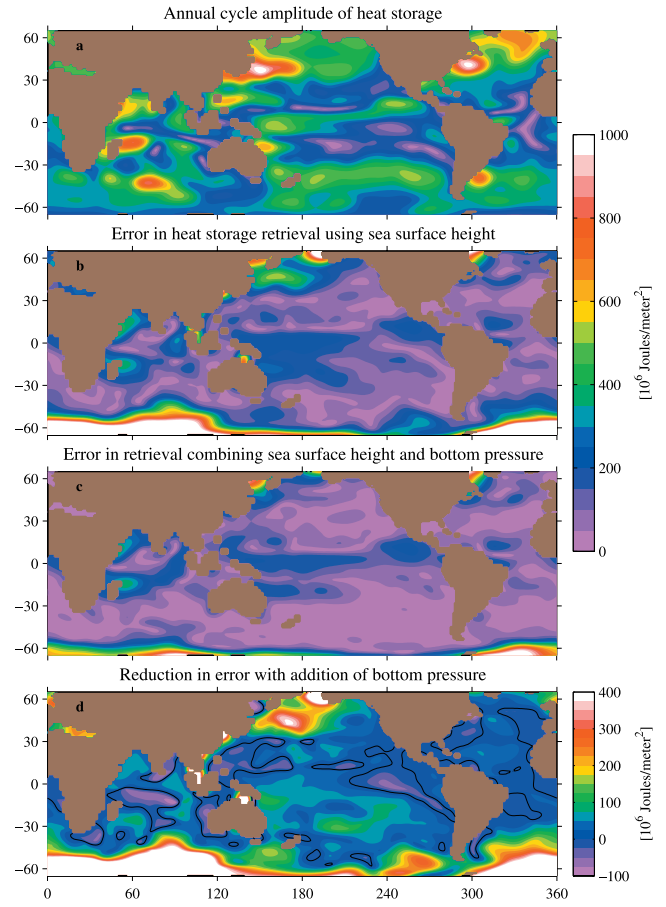


Figure 4. (a) Amplitude of the annual cycle of heat storage from the model. (b) RMS error in heat storage calculated using sea surface height alone. (c) Error in heat storage when using sea surface height combined with bottom pressure. (d) RMS difference in the errors when using sea surface height alone and when combined with bottom pressure.

1995], and indeed this has allowed the technique to be widely used to accurately observe tropical heat storage changes associated with El Niño. In the high latitudes, however, the estimates are quite poor, with error levels exceeding the actual level of variability there. When the bottom pressure is included in the calculation combined with the sea surface height in (26), the results are improved (Figure 3c), as is expected since the barotropic variability has now been corrected for. Figure 3d shows the reduction in the error between the case when the sea surface height is used alone and when it is combined with bottom pressure. Even with the inclusion of the bottom pressure in the heat content estimation, there are still errors from the neglect of the haline contribution to steric height as well as the inaccuracy of using a depth-independent thermal expansion coefficient. Observational errors in the sea surface height and gravity data, etc. were not included in these figures, but will be discussed and quantified in section 5.

[30] The monthly values of true and estimated heat storage were fit to an annual cycle, a semiannual cycle and a linear trend, in order to identify if the timescale of the phenomena affects the recovery of the heat storage. The results are shown in Figures 4 and 5. The annual and

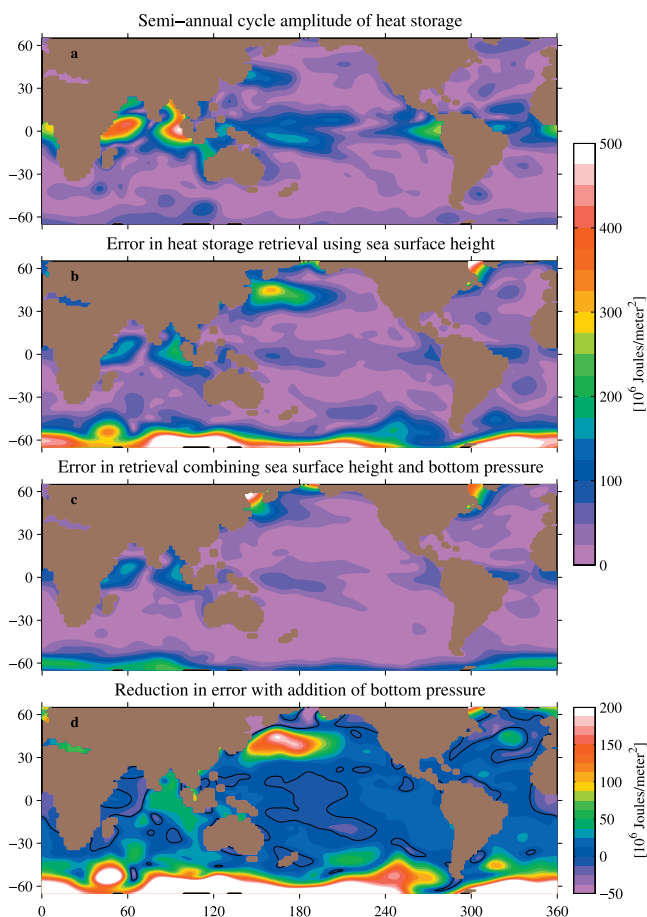


Figure 5. (a) Amplitude of the semiannual cycle of heat storage from the model. (b) RMS error in heat storage calculated using sea surface height alone. (c) Error in heat storage when using sea surface height combined with bottom pressure. (d) RMS difference in the errors when using sea surface height alone and when combined with bottom pressure.

semiannual cycles show improvements in line with those seen in the monthly maps (Figure 3). In particular, the annual cycle outside the tropics shows a rather poor recovery of heat storage from sea surface height alone (Figure 4b). The inclusion of bottom pressure largely corrects these deficiencies (Figure 4c). For the semiannual cycle, the heat storage variability is mostly confined to the tropics (Figure 5a), but the sea surface height alone would suggest large amount of variability in the high latitudes (Figure 5b), where there is actually very little. The improvements (Figures 5c and 5d) come mainly in the high latitudes where there are large barotropic motions expressed in the sea surface height. This is consistent with the high-frequency (timescales of days to a year) barotropic variability seen at high latitudes in altimetry and ocean models [Fu and Davidson, 1995; Fu and Smith, 1996; Fukumori et al., 1998; Tierney et al., 2000; Stammer et al., 2000; Webb and de Cuevas, 2002a, 2002b]. It should be noted that there are a few areas (Figures 3d, 4d, and 5d) where the addition of the bottom pressure leads to a slight increase in the estimated heat storage error. However, the error increases are small (less than $50 \times 10^6 \text{ J/m}^2$), and these areas are far

outweighed by the areas where the error is significantly reduced.

[31] The retrieval of the linear trend in heat storage (Figure 6), however, shows little to no improvement when bottom pressure is included. This is to be expected for several reasons. First, the linear trend in heat storage is associated with long-timescale phenomena which project on baroclinic modes and hence have weaker bottom pressure signals than the barotropic variability found at the annual and shorter timescales. Second, while the shorter period annual and semiannual cycles are associated with changes in heat storage largely confined above the thermocline, the linear trend in the model is showing drift in the deep ocean and so the assumption that α is constant over the depth of heating is not a good assumption. Also changes in salinity are probably playing a role on long timescale as well, and this is not accounted for in the present methodology.

5. Error Analysis

[32] There are different types of error sources that must be considered when evaluating the fidelity of retrieving time-

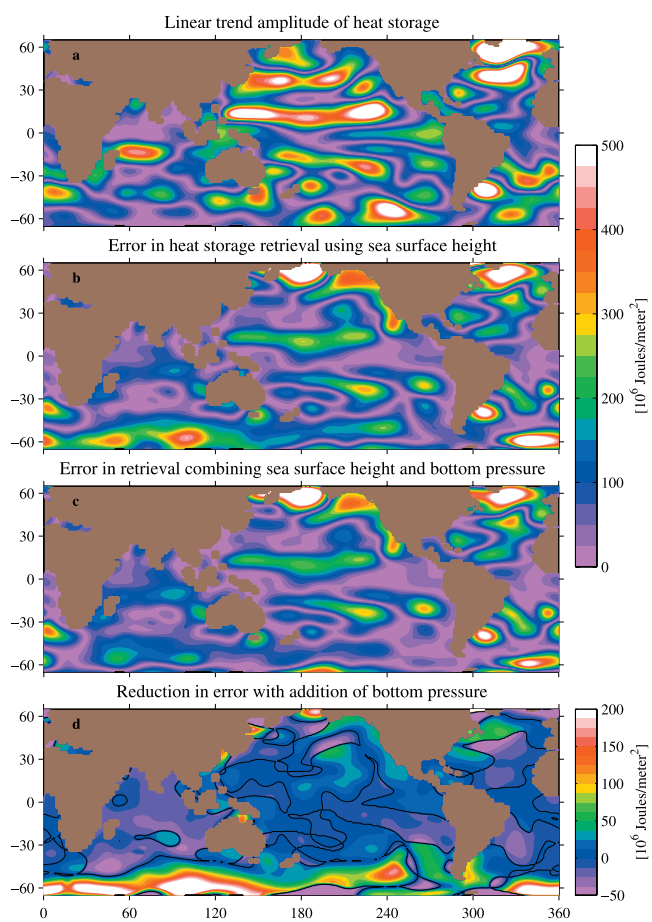


Figure 6. (a) Amplitude of the linear trend in heat storage from the model. (b) RMS error in heat storage calculated using sea surface height alone. (c) Error in heat storage when using sea surface height combined with bottom pressure. (d) RMS difference in the errors when using sea surface height alone and when combined with bottom pressure.

variable ocean heat content from altimetry and satellite gravity observations. There are measurement errors which arise from noise processes in the observation of sea surface height from the altimeters and bottom pressure from GRACE, and there are methodology errors which arise from the assumptions and simplifications that were made to arrive at (26) to estimate heat storage from the observable quantities. These can be further grouped into errors that are reduced by the introduction of the GRACE data, errors that are increased by using GRACE data and errors that are essentially unchanged. The quantitative error estimates in the following discussion are based on the ocean general circulation model output and a few ancillary data sets. The error propagation was performed using simulated GRACE and altimeter data based on the ocean model output; a global, gridded map of continental water storage over all regions except Antarctica from *Shmakin et al.* [2002]; of changes in snow mass over Antarctica using monthly, gridded, accumulation fields generated by the CSM-1 climate model developed at the National Center for Atmospheric Research [see, e.g., *Briegleb and Bromwich*, 1998]; of errors in atmospheric pressure over land (as by *Wahr et al.* [1998]); and of GRACE measurement errors, using error estimates provided by B. Thomas and M. Watkins (personal communication, 1998) [see also *Wahr et al.*, 1998; *Jet Propulsion Laboratory*, 2001]. While the numbers would vary if a different time period were analyzed or different forcing data sets were used, they do provide an assessment of the relative sizes of the different error sources. The reported errors represent the areal average over the ocean from 1° offshore of the coast within the latitude range 66°S to 66°N .

5.1. Measurement Errors

5.1.1. Altimetry Sampling Errors

[33] Altimetric measurements from TOPEX have high accuracy, with a point RMS error of about 3 cm [*Wunsch and Stammer*, 1998]. In this error analysis, we assume the majority of the error is due to residual orbit error. This assumption leads to the most pessimistic error estimate, since it assumes the measurement errors for a single satellite pass are correlated, so that spatial averaging does little to reduce them. Therefore, to estimate the number of independent samples within a given averaging disk, the number of degrees of freedom (N) was estimated using the weighted number of crossovers within the Gaussian average over a month time span. The number of crossovers within the Gaussian averaging area for a given time span is equal to the square of half the number of satellite passes. Averaged over a large area, such as that encompassed by a several hundred kilometer disk, these errors are reduced by $1/\sqrt{N}$. For a single month, this results in an average RMS error of $106 \times 10^6 \text{ J/m}^2$ in the retrieval of heat content (or equivalently, 40 W/m^2 in terms of a time rate of change of heat content) for a 500 km half-width averaging kernel. For 5 years of data, this source accounts for an error in the amplitude of the annual cycle of about 8 W/m^2 . This error source could be reduced somewhat by using multiple data sources (i.e., Jason plus Envisat and Geosat Follow-On); however, it is present whether or not GRACE data are used.

5.1.2. Inverted Barometer Correction Error

[34] One of the largest corrections made to the sea surface height measured from altimetry is for the inverted

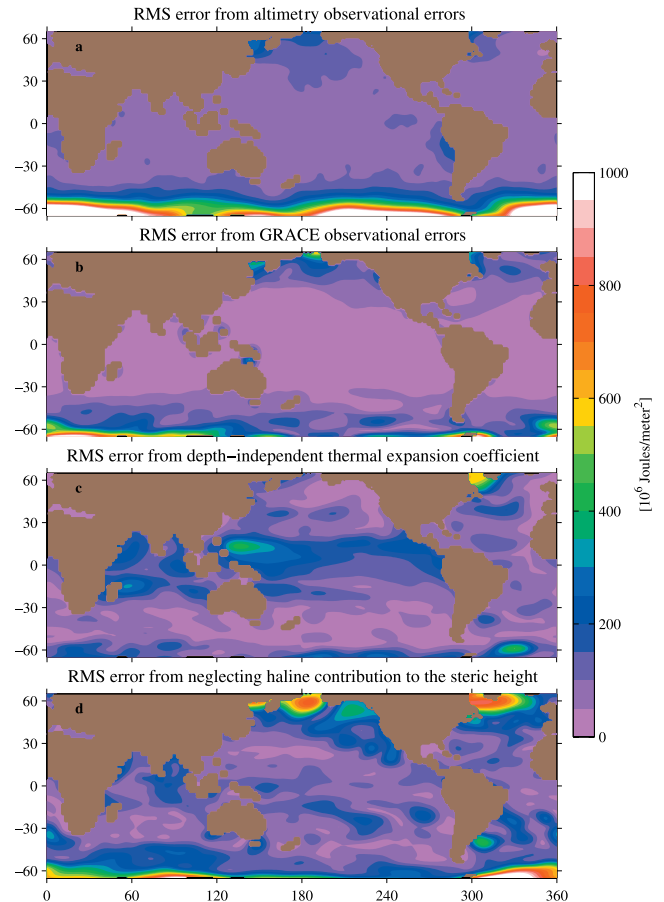


Figure 7. (a) The monthly RMS error arising from satellite altimetry errors sources. (b) The monthly RMS error arising from GRACE error sources. (c) The monthly RMS error from the thermal expansion coefficient. (d) The monthly RMS error from the neglect of the haline contribution to steric sea surface height.

barometer response of the ocean to atmospheric pressure variations [*Wunsch and Stammer*, 1997]. It is based on the mean sea level pressure derived from operational and reanalysis products from the National Center for Environmental Prediction (NCEP) or the European Centre for Medium-Range Weather Forecasts (ECMWF). These model products have errors and biases, but a detailed error estimation of these product's accuracy over the ocean has not been performed. However, over land the results indicate that the pressure is good to about 0.5 mbar [*Velicogna et al.*, 2001]. For the present purposes, as a measure of the error we take the RMS difference between the NCEP and ECMWF surface pressure products divided by $\sqrt{2}$, as by *Wahr et al.* [1998]. Translated into a heat storage error, errors in the inverted barometer correction introduce an RMS error of $77 \times 10^6 \text{ J/m}^2$ (29 W/m^2) for the monthly heat storage estimates, and 3 W/m^2 for the annual cycle. Figure 7a shows the monthly RMS of the heat content error arising from satellite altimetry errors sources, including errors in the inverted barometer and orbit error. The large errors, especially near Antarctica are due to errors in the inverted barometer correction.

5.1.3. GRACE Sampling Errors

[35] GRACE measurement errors are more complicated, as they are specified in spherical harmonic space. The purpose of the Gaussian spatial averaging we applied to the model data to generate Figures 3–5, is to reduce those errors to acceptable levels. For 5 years of data and a 500 km averaging radius, the RMS error in equivalent sea surface height is about 1 mm (Table 1), which results in an error in the monthly estimated heat storage of $20 \times 10^6 \text{ J/m}^2$ (8 W/m^2). The error in the annual cycle from this source is slightly less than 1 W/m^2 .

5.1.4. Postglacial Rebound

[36] The large postglacial rebound signal in the North Atlantic Ocean is problematic. Over the five year timescales we are considering, the postglacial rebound signal appears as a linear trend, so it will not affect the recovery of seasonal or other nonsecular signals. However, postglacial rebound is a significant source of error when trying to use GRACE data to examine the linear trend in bottom pressure. Unfortunately, the rebound is largest in the same places (i.e., the North Atlantic and Southern Oceans) where one might expect to see the largest signal in bottom pressure arising from secular changes in the ocean's baroclinic structure. The limited extent to which it can be modeled depends on the largely unknown viscosity profile of the Earth's mantle, and further research will be required to improve estimates of this error source. Taken together, all of the GRACE observation errors amount to $63 \times 10^6 \text{ J/m}^2$ (24 W/m^2) and the error in the annual cycle from GRACE observation errors is about 3 W/m^2 . Figure 7b shows the monthly RMS of the heat content error arising from satellite gravity errors, including errors in the GRACE estimated geoid and leakage from other signal such as the hydrology signal over land and post glacial rebound.

5.1.5. Leakage From Continental Hydrological Cycle

[37] Leakage from the large hydrology signal over land (e.g. groundwater storage) will contaminate the retrieval of GRACE signals close to the coast. However, coastal areas are also influenced by salinity effects from river runoff, and those effects have been ignored in our derivation of (21) and (26). Furthermore, the current generation of altimeters has poor data retrieval very close to the coasts. The implication, then, is that leakage of gravity signals from land will not be a large detriment to using the GRACE data. Furthermore, the contamination from the land hydrology can be significantly reduced using the methodology described by *Wahr et al.* [1998, equations (35)–(39)], and useful bottom pressure values GRACE will likely be obtainable to within about 100 km from the coast.

[38] It is important to understand the tradeoffs between the smoothing length scale and GRACE measurement errors, as well as the extent of the leakage from hydrological signals over land. Generally, the smaller the smoothing radius the better, as it improves spatial resolution, and reduces the area affected by leakage of the continental signals (though this signal can be significantly reduced as described by *Wahr et al.* [1998]). While the leakage of the hydrology signal over land is decreased by reducing the averaging radius, smaller averaging radii are associated with larger GRACE measurement errors. Therefore an optimal averaging area is problem dependent. To

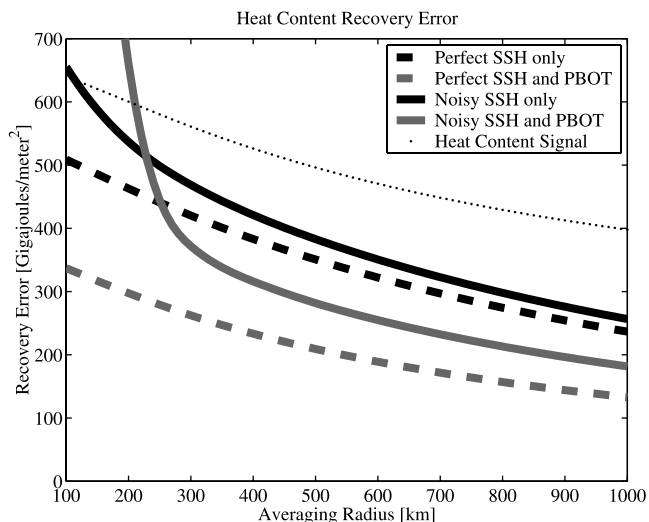


Figure 8. Error in heat storage estimate averaged over the global ocean as a function of the averaging radius.

illustrate the effect of the smoothing radius on the heat storage estimation errors, a range of smoothing radii from 100–1000 km were used to recompute the heat content retrieval error as a function of smoothing radius (Figure 8). Plotted are the globally averaged RMS of the heat content signal (dotted line), the estimated error using noise-free and noisy sea surface height alone (black dashed and solid lines respectively), and the estimated error using noise-free and noisy GRACE observations (gray dashed and solid line respectively). It is readily seen that in general the larger the averaging radius the lower the errors. However, at large averaging radii the time-varying heat content signal gets smeared out and weakened, and near the coasts the error from the hydrology signal leakage is increased. At the smallest averaging radii, GRACE measurement errors make the estimated heat content unusable. For the determination of heat storage, it is found that a 500-km averaging radius balances the errors introduced from altimetry and GRACE, while not leading to excessive contamination by the land hydrology signal, and not overly smoothing the desired heat content signal.

5.2. Methodology Errors

[39] Beyond the errors in estimation of heat storage from observational noise sources, there are errors introduced due to some of the assumptions made.

5.2.1. Thermal Expansion Coefficient Errors

[40] The thermal expansion coefficient is not constant over the depth that the heating is occurring as was assumed in deriving (18). Furthermore, α was calculated from the monthly mean sea surface temperature and salinity. When real data from the GRACE mission is available along with altimeter data from the ongoing missions, the thermal expansion coefficient will be calculated from the climatological surface temperature and salinity fields [*Levitus et al.*, 1994; *Levitus and Boyer*, 1994] or remotely sensed sea surface temperature [i.e., *Reynolds and Smith*, 1994]. These assumptions introduce errors into the estimation of the heat

storage. We use the model output for α and T , and estimate the error as

$$H'_{err}(\theta, \phi, t) = \frac{\rho C_p}{\alpha_0} \left[\int_{-h}^{\eta} \alpha(\theta, \phi, z, t) T'(\theta, \phi, z, t) dz - \alpha_0(\theta, \phi, t) \int_{-h}^{\eta} T(\theta, \phi, z, t) dz \right] \quad (27)$$

We find that the assumption of a depth independent thermal expansion coefficient introduces a globally averaged RMS error in the monthly estimated heat storage of $109 \times 10^6 \text{ J/m}^2$ (41 W/m^2) and the error in the estimated annual cycle for 5 years of data is about 10 W/m^2 . The contribution to the error budget from the assumption of a depth independent thermal expansion coefficient is shown in Figure 7c.

5.2.2. Haline Effects

[41] The contribution to the steric sea surface height by haline contraction was also neglected in the estimation procedure, introducing another error source. The contribution to the error budget from this assumption is estimated as,

$$H'_{err}(\theta, \phi, t) = \frac{\rho C_p}{\alpha_0} \int_{-h}^{\eta} \beta S' dz. \quad (28)$$

The neglect of the haline contribution to the steric sea surface height contributes an error of about $139 \times 10^6 \text{ J/m}^2$ (53 W/m^2) and the error in the annual cycle is about 11 W/m^2 . Figure 7d shows the monthly RMS of the error arising from the neglect of the haline contribution to the steric sea surface height.

[42] Taken together, the methodology errors account for an error of about 15 W/m^2 in the estimate of the annual cycle. The errors inherent in the methodology then account for about 3 times the error variance introduced by the total of the observational errors at 9 W/m^2 . Overall, this indicates that the estimation of heat storage using a 500 km averaging radius will not be vastly improved by either additional sea surface height data or from more precise satellite gravity observations. Rather, observations of salinity (either remotely sensed or in situ) would be of most benefit. Modification of the estimation methodology to break the constraint of a depth independent thermal expansion coefficient would also be of benefit. If GRACE performs to specification, it is expected that higher-precision satellite gravity missions will be flown in the future. This increased precision would allow for a decreased smoothing radius, and therefore permit higher spatial resolution in the heat storage estimates.

6. Conclusions

[43] The combination of satellite altimetry combined with bottom pressure observations (i.e., from the GRACE mission) offers a superior method for estimating the ocean's time-varying heat storage over using altimetry alone. Specifically, it significantly reduces errors associated with barotropic variability at high latitudes, which would otherwise dominate the errors in the inferred steric height variability in those regions. For the month-to-month variations in heat storage, with a 500 km half-width averaging

kernel, the error in the estimated heat content from altimetry alone is about $380 \times 10^6 \text{ J/m}^2$ compared to $200 \times 10^6 \text{ J/m}^2$ for the heat content computed from hydrographic profiles. When bottom pressure observations from satellite gravity are included, the error is reduced to $280 \times 10^6 \text{ J/m}^2$, more comparable to using hydrography. However, while the addition of bottom pressure data does significantly reduce the errors in the estimated heat content, there are still significant limitations that must be addressed before this methodology can equal the accuracy of in situ measurements. In particular, the addition of salinity observations, either in situ or remotely sensed, would be of great benefit.

[44] The challenge now will be to combine in situ observations of temperature and salinity from the profiling floats to be used in the Argo float program [Roemmich and Owens, 2000] to provide ground truth by which to test the method described here. Furthermore, satellite altimetry, GRACE and Argo will complement each other to provide a more complete Global Ocean Observing System. The in situ observations from the Argo floats should allow more accurate calculation of the thermal expansion coefficient, as well as take into account the haline effects in the steric sea surface height. However, the float data will suffer from sparse coverage and eddy aliasing problems. At the same time, the satellite observations should allow for a more complete spatial coverage to fill in gaps in the float data. So the combination should provide a more complete and reliable measure of the ocean heat storage. The resulting estimates of heat storage will place a strong constraint and consistency check on the estimates of surface heat flux produced by the meteorological centers. Taken together, the addition of GRACE to the ocean observation system will improve the estimation of the time-varying heat storage and play a fundamental role in the Global Climate Observing System being deployed.

[45] **Acknowledgments.** We would like to thank Andrey Shmakin, Chris Milly, and Krista Dunne for providing the output of their global, gridded water storage data set; and Dazhong Han for providing his elastic Love numbers. This work was partially supported by NASA grant NAG5-7703 and JPL contract 1218134 to the University of Colorado, JPL contract 1234336 to the Woods Hole Oceanographic Institution, and by the NSF through its sponsorship of NCAR. This is Woods Hole Oceanographic Institution Contribution number 10840.

References

- Briegleb, B. P., and D. H. Bromwich, Polar climate simulation of the NCAR CCM3, *J. Clim.*, *11*, 1270–1281, 1998.
- Chambers, D. P., B. D. Tapley, and R. H. Stewart, Long-period ocean heat storage rates and basin-scale heat fluxes from TOPEX, *J. Geophys. Res.*, *102*, 10,525–10,533, 1997.
- Chambers, D. P., B. D. Tapley, and R. H. Stewart, Measuring heat-storage changes in the Equatorial Pacific: A comparison between TOPEX altimetry and TAO buoys, *J. Geophys. Res.*, *103*, 18,591–18,597, 1998.
- Chao, B. F., and R. S. Gross, Changes in the Earth's rotation and low-degree gravitational field induced by earthquakes, *Geophys. J. R. Astron. Soc.*, *91*, 569–596, 1987.
- Chao, Y., and L.-L. Fu, A comparison between the TOPEX/Poseidon data and a global ocean general circulation model during 1992–1993, *J. Geophys. Res.*, *100*, 24,965–24,976, 1995.
- Chen, J. L., C. K. Shum, C. R. Wilson, D. P. Chambers, and B. D. Tapley, Seasonal sea level change from TOPEX/Poseidon observations and thermal contribution, *J. Geodesy*, *72*, 638–647, 2000.
- Cheney, R. E., L. Miller, R. Agreen, N. Doyle, and J. Lillibridge, TOPEX/Poseidon: The 2-cm solution, *J. Geophys. Res.*, *99*, 24,555–24,564, 1994.

- Dickey, J. O., et al., *Satellite Gravity and the Geosphere: Contributions to the Study of the Solid Earth and Its Fluid Envelope*, Natl. Acad. Press, Washington, D.C., 1997.
- Dukowicz, J., and R. D. Smith, Implicit free-surface method for the Bryan-Cox-Semtner ocean model, *J. Geophys. Res.*, *99*, 7991–8014, 1994.
- Farrell, W. E., Deformation of the Earth by surface loads, *Rev. Geophys.*, *10*, 761–797, 1972.
- Ferry, N., G. Reverdin, and A. Oschlies, Seasonal sea surface height variability in the North Atlantic Ocean, *J. Geophys. Res.*, *105*, 6307–6326, 2000.
- Fu, L.-L., and D. B. Chelton, Large-scale ocean circulation, in *Satellite Altimetry and Earth Sciences*, edited by L.-L. Fu and A. Cazenave, pp. 133–169, Academic, San Diego, Calif., 2001.
- Fu, L.-L., and R. A. Davidson, A note on the barotropic response of sea level to time-dependent wind forcing, *J. Geophys. Res.*, *100*, 24,955–24,963, 1995.
- Fu, L.-L., and R. D. Smith, Global ocean circulation from satellite altimetry and high-resolution computer simulation, *Bull. Am. Meteorol. Soc.*, *77*, 2625–2636, 1996.
- Fukumori, I., R. Raghunath, and L.-L. Fu, Nature of global large-scale sea level variability in relation to atmospheric forcing: A modeling study, *J. Geophys. Res.*, *103*, 5493–5512, 1998.
- Gent, P. R., and J. C. McWilliams, Isopycnal mixing in ocean circulation models, *J. Phys. Oceanogr.*, *20*, 150–155, 1990.
- Gill, A. E., *Atmosphere-Ocean Dynamics*, Academic, San Diego, Calif., 1982.
- Gill, A. E., and P. P. Niiler, The theory of the seasonal variability in the ocean, *Deep Sea Res.*, *20*, 141–178, 1973.
- Greatbatch, R. J., A note on the representation of steric sea level in models that conserve volume rather than mass, *J. Geophys. Res.*, *99*, 12,767–12,771, 1994.
- Hendricks, J. R., R. R. Leben, G. H. Born, and C. J. Koblinsky, Empirical orthogonal function analysis of global TOPEX/Poseidon altimeter data and implications for detection of global sea level rise, *J. Geophys. Res.*, *101*, 14,131–14,145, 1996.
- Hughes, C. W., C. Wunsch, and V. Zlotnicki, Satellite peers through the oceans from space, *Eos Trans. AGU*, *81*, 68, 2000.
- Jekeli, C., Alternative methods to smooth the Earth's gravity field, *Tech. Rep. 327*, Dep. of Geod. Sci. and Surv., Ohio State Univ., Columbus, 1980.
- Jet Propulsion Laboratory, GRACE science and mission requirements document, GRACE 327-200, Rev. D, *Tech. Rep. JPL Publ. D-15928*, Jet Propul. Lab., Pasadena, Calif., 2001.
- Johnson, T. J., C. R. Wilson, and B. F. Chao, Nontidal oceanic contributions to gravitational field changes: Predictions of the Parallel Ocean Climate Model, *J. Geophys. Res.*, *106*, 11,315–11,334, 2001.
- Large, W. G., J. C. McWilliams, and S. C. Doney, Oceanic vertical mixing: A review and a model with nonlocal boundary layer parameterization, *Rev. Geophys.*, *32*, 363–403, 1994.
- Large, W. G., G. Danabasoglu, S. Doney, and J. C. McWilliams, Sensitivity to surface forcing and boundary layer mixing in a global ocean model: Annual mean climatology, *J. Phys. Oceanogr.*, *27*, 2418–2447, 1997.
- Leuliette, E. W., and J. M. Wahr, Coupled pattern analysis of sea surface temperature and TOPEX/Poseidon sea surface height, *J. Phys. Oceanogr.*, *29*, 599–611, 1999.
- Levitus, S., and T. Boyer, *World Ocean Atlas 1994*, vol. 4, *Temperature*, NOAA Atlas NESDIS, vol. 4, 129 pp., Natl. Oceanic and Atmos. Admin., Washington, D.C., 1994.
- Levitus, S., R. Burgett, and T. Boyer, *World Ocean Atlas 1994*, vol. 3, *Nutrients*, NOAA Atlas NESDIS, vol. 3, 129 pp., Natl. Oceanic and Atmos. Admin., Washington, D.C., 1994.
- Maes, C., Estimating the influence of salinity of sea level anomaly in the ocean, *Geophys. Res. Lett.*, *25*, 3551–3554, 1998.
- Polito, P. S., O. T. Sato, and W. T. Liu, Characterization and validation of heat storage variability from TOPEX/Poseidon at four oceanographic sites, *J. Geophys. Res.*, *105*, 16,911–16,921, 2000.
- Ponte, R. M., A preliminary model study of the large-scale seasonal cycle in bottom pressure over the global ocean, *J. Geophys. Res.*, *104*, 1289–1300, 1999.
- Repert, J. P., J. R. Donguy, G. Elden, and K. Wyrski, Relations between sea level, thermocline depth, heat content, and dynamic height in the tropical Pacific Ocean, *J. Geophys. Res.*, *90*, 11,719–11,725, 1985.
- Reynolds, R. W., and T. M. Smith, Improved global sea surface temperature analyses using optimum interpolation, *J. Clim.*, *7*, 929–948, 1994.
- Roemmich, D., and W. B. Owens, The argo project: Global ocean observations for understanding and prediction of climate variability, *Oceanography*, *13*, 45–50, 2000.
- Sato, O. T., P. S. Polito, and W. T. Liu, Importance of salinity measurements in the heat storage estimation from TOPEX/Poseidon, *Geophys. Res. Lett.*, *27*, 549–551, 2000.
- Shmakin, A. B., P. C. D. Milly, and K. A. Dunne, Global modeling of land water and energy balances, 3, Interannual variability, *J. Hydrometeorol.*, *3*, 311–321, 2002.
- Smagorinsky, J., General circulation experiments with the primitive equations, I, The basic experiment, *Mon. Weather Rev.*, *91*, 99–164, 1963.
- Smith, R. D., and J. C. McWilliams, Anisotropic horizontal viscosity for ocean models, *Ocean Modell.*, *5*, Hooke Inst., Oxford Univ., Oxford, U. K., 2002.
- Stammer, D., Steric and wind-induced changes in TOPEX/Poseidon large-scale sea surface topography observations, *J. Geophys. Res.*, *102*, 20,987–21,009, 1997.
- Stammer, D., C. Wunsch, and R. Ponte, De-aliasing of global high frequency barotropic motions in altimeter observations, *Geophys. Res. Lett.*, *27*, 1175–1178, 2000.
- Swenson, S., and J. Wahr, Methods for inferring regional surface-mass anomalies from Gravity Recovery and Climate Experiment (GRACE) measurements of time-variable gravity, *J. Geophys. Res.*, *107*(B9), 2193, doi:10.1029/2001JB000576, 2002.
- Tierney, C., J. Wahr, F. Bryan, and V. Zlotnicki, Short-period oceanic circulation: Implications for satellite altimetry, *Geophys. Res. Lett.*, *27*, 1255–1258, 2000.
- Tomczak, M., and J. S. Godfrey, *Regional Oceanography: An Introduction*, Pergamon, New York, 1994.
- Velicogna, I., J. Wahr, and H. Van den Dool, Can surface pressure be used to remove atmospheric contributions from GRACE data with sufficient accuracy to recover hydrological signals?, *J. Geophys. Res.*, *106*, 16,415–16,434, 2001.
- Vivier, F., K. A. Kelly, and L. Thompson, Contributions of wind forcing, waves and surface heating to sea surface height observations in the Pacific Ocean, *J. Geophys. Res.*, *104*, 20,767–20,788, 1999.
- Wahr, J., M. Molenaar, and F. Bryan, Time variability of the Earth's gravity field: Hydrological and oceanic effect and their possible detection using GRACE, *J. Geophys. Res.*, *103*, 30,205–30,229, 1998.
- Wahr, J. M., S. R. Jayne, and F. O. Bryan, A method of inferring changes in deep ocean currents from satellite measurements of time variable gravity, *J. Geophys. Res.*, doi:10.1029/2001JC001274, in press, 2002.
- Wang, L., and C. Koblinski, Can the TOPEX/Poseidon altimetry data be used to estimate air-sea heat flux in the North Atlantic, *Geophys. Res. Lett.*, *24*, 139–142, 1997.
- Webb, D. J., and B. A. de Cuevas, An ocean resonance in the southeast Pacific, *Geophys. Res. Lett.*, *29*(14), 1252, doi:10.1029/2001GL014259, 2002a.
- Webb, D. J., and B. A. de Cuevas, An ocean resonance in the Indian sector of the Southern Ocean, *Geophys. Res. Lett.*, *29*(14), 1664, doi:10.1029/2002GL015270, 2002b.
- White, W. B., and C.-K. Tai, Inferring interannual changes in the global upper ocean heat storage from TOPEX altimetry, *J. Geophys. Res.*, *100*, 24,943–24,954, 1995.
- Wunsch, C., and D. Stammer, Atmospheric loading and the oceanic “inverted barometer” effect, *Rev. Geophys.*, *35*, 79–107, 1997.
- Wunsch, C., and D. Stammer, Satellite altimetry, the marine geoid, and the oceanic general circulation, *Annu. Rev. Earth Planet. Sci.*, *26*, 219–253, 1998.

F. O. Bryan, Climate and Global Dynamics Division, National Center for Atmospheric Research, PO Box 3000, Boulder, CO 80307-3000, USA. (bryan@ucar.edu)

S. R. Jayne, Physical Oceanography Department, Woods Hole Oceanographic Institution, MS 21, Woods Hole, MA 02543-1541, USA. (sjayne@whoi.edu)

J. M. Wahr, Department of Physics, University of Colorado, Campus Box 390, Boulder, CO 80309-0390, USA. (wahr@lemond.colorado.edu)